Int J Adv Manuf Technol (2016) 85:2839–2845
DOI 10.1007/s00170-015-8091-1

ORIGINAL ARTICLE

Energy consumption characterization in precision hard machining using CBN cutting tools

Wit Grzesik [1] · Berend Denkena [2] · Krzysztof Żak [1] · Thilo Grove [2] · Benjamin Bergmann [2]

Received: 28 July 2015 / Accepted: 9 November 2015 / Published online: 25 November 2015

Abstract In this paper, the contribution of tool wear to the energy balance was determined for precision hard turning using chamfered CBN cutting tools. The tool nose wear VB_C and the corresponding changes of component forces F_c, F_f and F_p resulting from tool wear evolution were continuously measured during wear tests. Based on the cutting mechanics, specific cutting and ploughing energies were calculated for a number of tool wear states. In particular, changes of energy balance due to tool wear under variable feed rate, depth of cut and tool nose radius were discussed. A distinction between material removal conditions resulting from precision cutting and grinding at a very low uncut chip thickness is considered.

Keywords Hard machining · CBN tool · Tool wear · Cutting energy · Ploughing energy

✉ Krzysztof Żak
k.zak@po.opole.pl

Wit Grzesik
w.grzesik@po.opole.pl

Berend Denkena
Denkena@ifw.uni-hannover.de

Thilo Grove
grove@ifw.uni-hannover.de

Benjamin Bergmann
bergmannifw@uni-hannover.de

[1] Opole University of Technology, Opole, Poland

[2] Gottfried Wilhelm Leibniz Universität Hannover, Hannover, Germany

1 Introduction

Hard machining has been established a leading machining technology for various machine components made of hardened steels, such as geared shafts, bearing and hydraulic components, which replaces or assists grinding operations [1, 2]. Predominantly, scientific and engineering issues of hard turning cover such problems as cutting mechanics, chip formation, tool wear, surface integrity and part accuracy [3–5]. Unfortunately, energy balance in hard machining resulting from the specific action of the cutting edge has not been investigated in a satisfactory manner, but it seems to be an important objective of hard machining research. Moreover, more work is needed to optimize energy usage in metal cutting besides economic objectives because it is a process with large energy consumption and low energy efficiency [6, 7]. In case of hard machining, the energy consumption increases distinctly due to extreme high hardness of the material machined and high negative rake angle of the CBN cutting tool used. In addition, tool wear should evidently influence friction and intensify ploughing action of the cutting edge. In general, hard machining is distinguished by dominating radial (passive) force in comparison to conventional turning for which the radial force F_r=(0.3–0.5) F_c. Consequently, the radial force cannot be neglected in characterizing static and dynamic behaviour of the machining system. This rule is also valid for tool wear evolution, especially when machining with tools of large nose radius of 800 and 1200 μm [8]. In particular [4, 9], CBN tools with large negative chamfer angles cause the increase in the passive force and more intensive ploughing action which produces higher friction and wear and reduces tool life. Similarly, tool nose radius affects uncut chip geometry that increases ploughing forces in the hard turning process [10]. In this study, energy consumed in hard turning of 16MnCrS5 (AISI 5115) hardened steel with worn CBN tools under the variable

feed rate, the depth of cut and tool nose radius was determined based on measurements of the component forces F_c, F_f and F_p during tool wear [8]. The obtained values of the specific cutting energy corresponding to the three process variables were mapped in the diagram showing its dependence on the undeformed chip thickness [11].

2 Mechanics of the machining process

2.1 Geometry of cross-sectional area of cut

In finish hard turning, the depth of cut (a_p) is generally smaller than the nose radius (r_ε) and the cross-sectional area of cut has a comma shape as shown in Fig. 1a. Consequently, the cutting ratio b/h is higher than 1. The cross-sectional area for such a case of cutting is described by the effective contact length l_k and the average undeformed chip thickness (UCT) h_m. In addition, the effective tool edge angle κ_{re} is defined when replacing a curvilinear cutting edge being a part of the nose by an equivalent straight cutting edge (ECE) shown in Fig. 1b.

Geometrical quantities (the cutting tool angle κ_{re}, the contact length l_k, the average UCT h_m, the area of cut A_{nc}) are expressed by a set of equations (1.1–1.4), as follows:

$$\kappa_{re} = \frac{1}{2}\arccos\left(\frac{r_\varepsilon - a_p}{r_\varepsilon}\right) \tag{1.1}$$

$$l_k = 2\kappa_{re} r_\varepsilon \tag{1.2}$$

$$h_m = a_p f / l_k \tag{1.3}$$

$$A_{nc} = l_k h_m \tag{1.4}$$

2.2 Components of the resultant cutting force and total energy

Measurements of three components of the resultant cutting force were performed in the *xyz* coordinate system as shown in Fig. 1a. Specific cutting e_c and ploughing e_p energies are calculated based on the equivalent cutting edge of the length l_k as

$$e_c = F_c / A_{nc} \tag{2.1}$$

$$e_p = F_p / A_{nc} \tag{2.2}$$

2.3 Experimental details

This study concerns external cylindrical turning of a case-hardened 16MnCrS5 (AISI 5115) steel with the average micro-hardness of 850–800 $HV_{0.05}$ performed on a CNC lathe Gildemeister CTX 520 linear. Both chemical composition and physical properties of the workpiece material are specified in Tables 1 and 2, respectively. CBN cutting tools, grade WBN 560 by *CeramTec*, with 56 % CBN content and an average grain size of 3 μm were used. The effective rake angle was $\gamma_{ne}=-24°$, and the chamfer angle was $\gamma_{fe}=-30°$. The clearance angle $\alpha_n=6°$ and the inclination angle $\lambda_s=-6°$. Furthermore, the cutting edge radius was kept constant at $r_\beta=8$ μm. The cutting speed was constant at 150 m/min. On the other hand, three feed rates $f=10$, 100 and 200 μm; three depths of cut $a_p=10$, 100 and 200 μm; and four tool nose radii $r_\varepsilon=100$, 400, 800 and 1200 μm were selected as variable factors. This means that the effective tool edge angle κ_{re} and the average UCT h_m vary according to Eqns. 1.1 and 1.3. The corresponding values of the effective tool edge angle κ_{re} and the average UCT h_m determined by Eqns. 1.1 and 1.3 are specified in Table 3.

Accordingly, the resolution of the resultant cutting force F into three components F_z, F_y and F_x shown in Fig. 1a is different depending on the cutting arrangement. The resultant force components were measured using a three-component piezoelectric dynamometer Kistler—model 9121. The measured signals were processed with a sampling rate of $f=$ 1 kHz and a low-pass filter with a cut-off frequency of $f_c=$ 300 Hz [8].

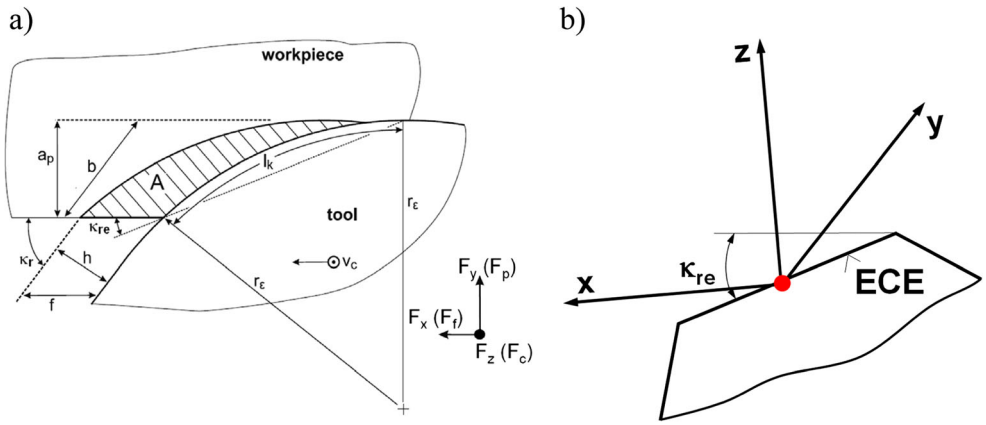

Fig. 1 Description of the cross-sectional area (**a**) and equivalent cutting edge (ECE) (**b**)

Table 1 Specification of chemical composition of 16MnCrS5 (AISI 5115) steel

C	Mn	Cr	Si	P	S
0.14–0.19	1.0–1.3	0.8–1.1	0–0.4	0–0.025	0–0.035

From [12]

Wear tests were conducted to achieve the limited value of VB_C ≈200 μm [8]. Using the methodology described in Sect. 2, the changes of specific energies during all nine sets of wear tests were determined. As mentioned in Sect. 1, the own research findings concerning tool wear coincide, in trends, to the literature reports. In general, the main tool wear mechanisms involved in CBN hard turning are caused by abrasion, adhesion and diffusion depending on the thermal loading, binder phase and chemical stability of CBN tools [13]. However, mechanical wear dominates at low cutting speed and thermal wear at high cutting speed. As a result, the representative tool wear indicator measured in the tool wear tests was VB_C. Also, tool wear patterns are similar to those reported in the literature related to finish CBN machining when abrasive wear of tool nose covers the flank (mainly) and the rake (chamfer) faces. In case of low content CBN tools (56 % CBN phase) used, the dominant wear patterns observed create tool nose wear with characteristic ellipsoidal shape as shown in Fig. 2.

3 Results and discussion

3.1 Changes of cutting forces with tool wear

Figure 3 shows an exemplary case of force evolutions recorded during tool wear keeping the feed rate at 100 μm, the depth of cut at 100 μm and the tool corner radius at 800 μm. For this set of variable machining parameters, the UCT is equal to about 25 μm (see Table 1) and represents its medium value. It should be noted that the ploughing action and the accompanying spring-back effect and severe sliding friction are intensified when hard machining with very low UCT value, as, for example, equal to 2.5 μm (ten times lower than previously) when the smallest feed of 10 μm was applied. The tool-workpiece reaction is that the passive force reaches the highest value of about 130 N (see course #3 vs. #2 in Fig. 4) for fresh tool, and its value rises distinctly during tool wear. In addition, for a such specific cutting arrangement, the ratio of h/r_β is about 0.3. In comparison, according to Kragelski's formula, chip formation under dry cutting conditions occurs when h/r_β=0.1–0.2. Moreover, for the maximum UCT value of about 64 μm (r_ε=100 μm, f=100 μm, a_p=100 μm), the h/r_β=8, which means that the ploughing action is distinctly reduced (see course #1 in Fig. 4c). It is evident in Fig. 3 that the passive force F_p is the dominant force component and its value increases mostly during tool wear. For instance, the F_p force rises from about 80 N for fresh cutting tools to about 130 N for worn tools. However, the rise of F_c force is more intensive than feed force F_f.

In general, according to graphs presented in Fig. 4, the highest rise of the F_p force was observed for the maximum feed rate of 200 μm (Fig. 4a), the maximum corner radius of 1200 μm (Fig. 4b) and the minimum depth of cut of 10 μm (Fig. 4c). An excessive rise of the F_c and F_f forces during tool wear was observed for the lowest corner radius of 100 μm [8].

The tool wear is a random phenomenon in nature, especially when tool wear test is very long (about 90 min in this study). Such tool wear behaviour can results in an unpredictable change of measured VBc indicator which rather occurs in the second part of tool wear test. As a result, tool wear increment in the time unit can change for course #1 as in Fig. 4b. In this case study with the smallest tool nose radius of 100 μm, the natural change due to wear is its increase, so a new tool with higher nose radius is created. Finally, tool wear can increase more intensively.

3.2 Changes of cutting and ploughing energies with tool wear

The basic goal of this study was to characterize the evolution of tool wear in terms of the specific cutting energy (e_c) and the ploughing energy (e_p) consumed. The specific cutting energy

Table 2 Specification of physical properties of 16MnCrS5 (AISI 5115) steel as received

Hardness (delivery condition)	Max. 217 HB			
Tensile strength Rm (as-received condition)	Approx. 720 MPa			
Working hardness	Max. 60 HRC (surface hardness)			
Thermal expansion coefficient (10^{-6} m/(m K))	20–100 °C	20–200 °C	20–300 °C	20–400 °C
	11.5	12.5	13.3	13.9
Thermal conductivity (W/(m K))	20 °C			
	44.0			

From [12]

Table 3 Specification of values of κ_{re} and h_m

Tool nose radius r_ε (μm)	Feed rate, f (μm)	Depth of cut, a_p (μm)	Cutting speed (m/min)	Effective tool edge angle, κ_{re} (°)	Average UCT h_m (μm)
100				45	63.7
400	100	100	150	21	34.6
800				14	24.7
1200				12	20.3
		10		5	7.9
800	100	100	150	14	24.7
		200		21	34.6
	10				2.5
800	100	100	150	14	24.7
	200				49.5

represents the energy required to remove the unit volume of material depending on the value of the cutting force F_c, whereas the specific ploughing energy represents the friction losses resulting from the action of the passive force F_p. Figure 5 shows the changes in energy balance during tool wear for variable feed rate, depth of cut and tool nose radius, respectively. It should be noted in Fig. 5b that the highest value of specific ploughing energy $e_p \approx 90$ GJ/m^3 was determined for the lowest feed $f=10$ μm and the lowest depth of cut $a_p=10$ μm at the end of tool wear test.

Changes of the components of specific energy and total specific energy as functions of the feed rate, nose radius and the depth of cut are presented in Fig. 5a–c, respectively. It was revealed that tool wear contributes mostly to the changes of specific ploughing energy rather than the specific cutting energy (Fig. 5b vs. Fig. 5a).

The general note is that in hard machining, the energy consumed for ploughing action of the tool over the hard surface predominantly overestimates the cutting energy (typically, the ratio e_c/e_p is lower than 1 and ranges between 0.5 and 0.8).

However, two specific cases can be distinguished in Figs. 4b and 5a: one when the ratio e_c/e_p oscillates around 1 for tools with the smallest nose radius of 100 μm and the second when the e_c/e_p decreases down to the minimum value of about 0.26 when the lowest depth of cut of 10 μm was applied. For the latter case, the specific ploughing energy is about four times higher than the specific cutting energy (88 vs. 23.3 GJ/m^3). As a result, the total specific energy determined as the sum of the e_c and e_p increases rapidly during tool wear for the minimum feed of 10 μm up to about 160 GJ/m^3 as shown in Fig. 5a. Less intensive increase of the e_t value is observed for the lowest depth of cut of 10 μm for which the maximum e_t value approaches 110 GJ/m^3. For other cases presented in Fig. 5c, the e_t value does not exceed 30 GJ/m^3. This energy amount is characteristic for steel grinding with extremely low UCT of 2 μm or lower [11].

3.3 Mapping of energy balance for different chip geometry

Figure 6 shows the map which compares specific cutting and total energies for different hard CBN turning operations and their evolution during tool wear. These are loge_t-logh_m graphs which highlight how the UCT influences the values of e_c and e_t for different machining parameters and tool corner radius. It should be noted that two data sets denoted by symbols 4 and 5 and 6 and 7 correspond to the tool corner radius of 800 μm

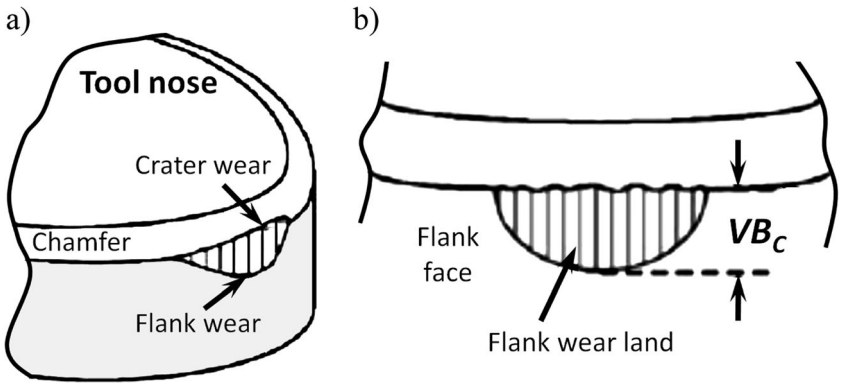

Fig. 2 Sketch showing worn nose of CBN tool used (**a**) and flank wear VB_C (**b**). After [13, 14] with modifications

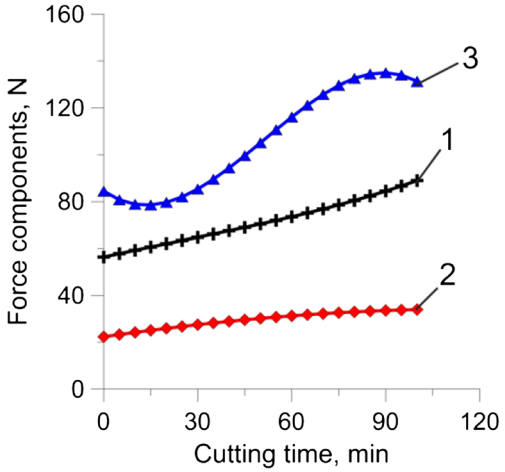

Fig. 3 Changes of force components during wear test. Cutting parameters: f=100 μm, a_p=100 μm, r_ε=800 μm. *1*—F_c; *2*—F_f; *3*—F_p

(h_m=24.7 μm) and 400 μm (h_m=34.6 μm), respectively. On the other hand, the maximum UCT of 63.7 μm corresponds to the minimum corner radius of r_ε=100 μm (bar #9).

In Fig. 6a, a line corresponding to both grinding and conventional cutting operations of alloy steels is marked in order to compare energy consumptions in hard and conventional (soft) turning operations. The boundary between grinding and cutting operations was selected at the UCT of 20 μm [11, 14]. It is interesting that for medium UCT values ranging from 20 to 50 μm, which corresponds to precision cutting [4], the values of the specific cutting energy related to the beginning of tool wear are lower than for conventional turning operations. However, an intensive ploughing action in hard machining causes that the total specific energy which aggregates both cutting and friction interactions exceeds substantially the specific energy in conventional machining, as depicted in Fig. 6b.

As discussed in Sect. 3.2 due to extremely small UCT in the range of several microns, the values of energy consumed when machining with the lowest feed rate of 10 μm and the lowest depth of cut of 10 μm (Fig. 5a) are typical for finish grinding of alloy steels, as presented in [11]. In these cases, the minimum UCT is equal to 2.5 and 7.9 μm, respectively (Fig. 6). It is interesting to note in Fig. 6 that a visible increase of e_t during tool wear is also obtained when the tool corner is equal r_ε=100 μm which corresponds to the maximum value of $h_{\min}$ of about 64 μm (bar #9).

Similar to the ploughing action caused by the passive force described in Sect. 4.1, the energy balance for different machining conditions is discussed in terms of the ratio of uncut chip thickness to the cutting edge radius (h/r_β). In this study, the ratio h/r_β increases from 0.3 for the minimum h of 2.5 μm to 8 for the maximum h of 64 μm. It is evident that the material removal conditions cause substantial differences in the ploughing action, associated spring-back effect and the cutting

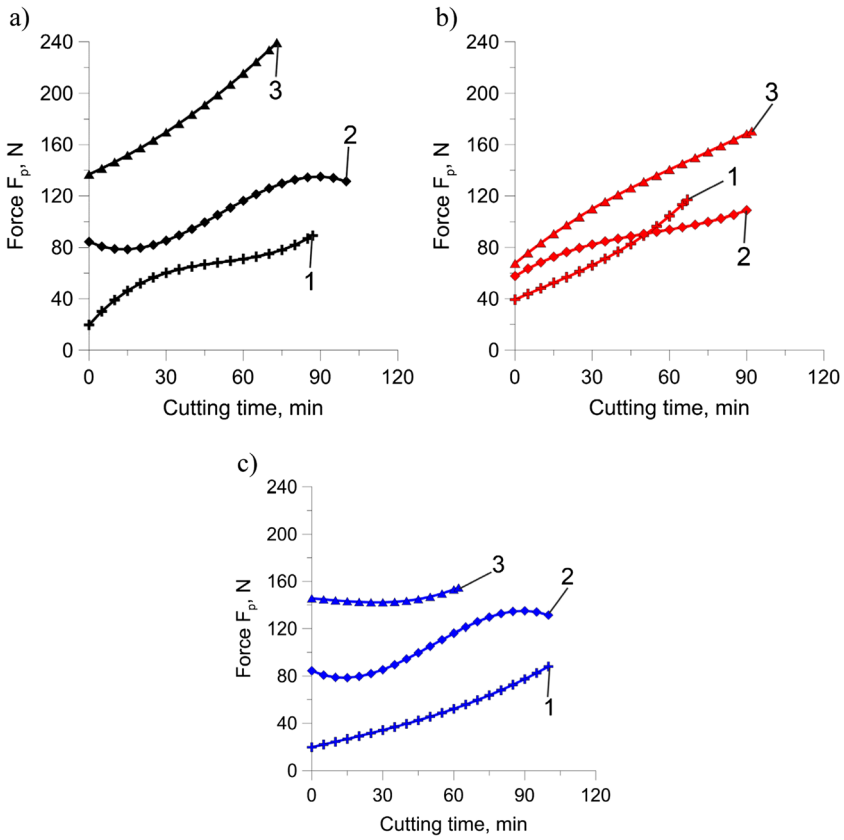

Fig. 4 Changes of passive force F_p for the following: **a** variable feed: 1–10, 2–100 and 3–200 μm; **b** variable corner radius: 1–100, 2–400 and 3–1200 μm; and **c** variable depth of cut: 1–10, 2–100 and 3–200 μm

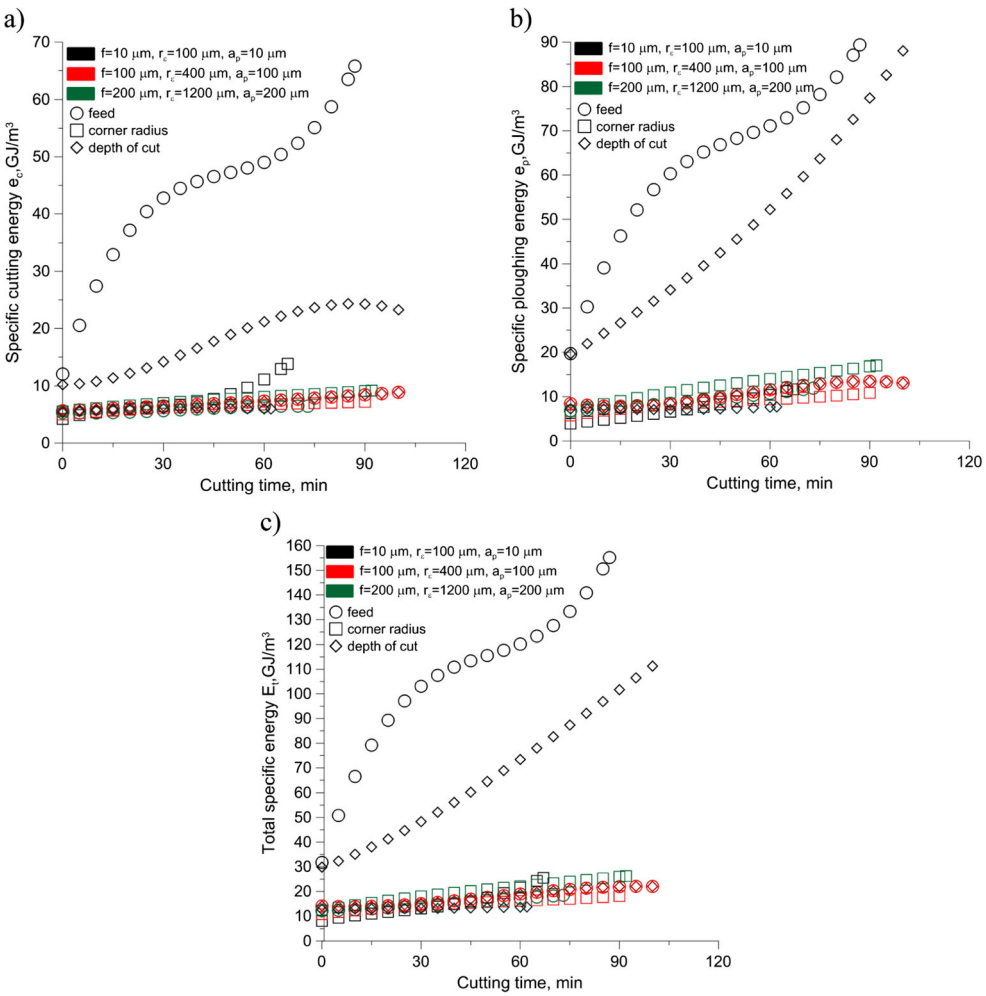

Fig. 5 Comparison of energy balance for different hard machining conditions used in this study: **a** specific cutting, **b** ploughing energy and **c** total energy

action. Taking into consideration finish conventional cutting for which the cutting edge radius typically ranges from 20 to 50 μm and the uncut chip thickness is typically higher than 100/200 μm (0.01/0.02 mm), i.e. the ratio h/r_β ranges from 2 to 5. These material removal conditions correspond to the hard machining performed with the maximum depth of cut of 200 μm (course #7 in Fig. 6a), the maximum feed rate of 200 μm (course #8 in Fig. 6a) and especially for the minimum tool nose radius of 10 μm (course #9 in Fig. 6a). The last case corresponds rather to broaching operations.

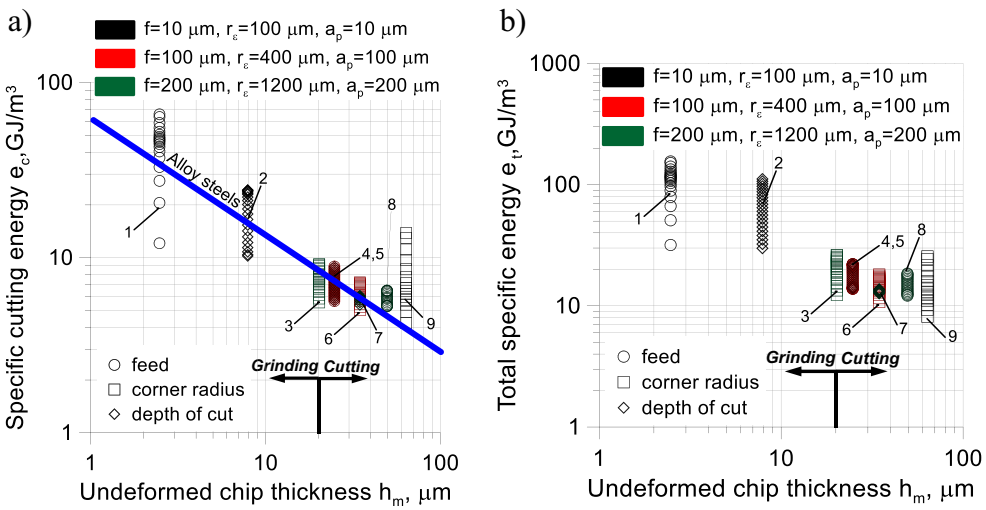

Fig. 6 The dependence of cutting (**a**) and total (**b**) specific energy on undeformed chip thickness. h_m: 1–2.5, 2–7.9, 3–20.3, 4.5–24.7, 6.7–34.6, 8–49.5 and 9–63.7 μm. Cutting parameters: *1*—f=10 μm, *2*—a_p=10 μm, *3*—r_ε=1200 μm, *4*—f=100 μm, *5*—a_p=100 μm, *6*—r_ε=400 μm, *7*—a_p=200 μm, *8*—f=200 μm and *9*—r_ε=100 μm

4 Conclusions

The following conclusions can be drawn based on the obtained results and their analysis:

- In CBN hard turning, the ploughing energy is generally higher than cutting energy. Only the e_c/e_p ratio is about 1 in the case of using tools with a very low nose radius.
- The cutting energy for lower feed rate and depth of cut is in the range characteristic for grinding with extremely low UCT of about 2 μm.
- The cutting energy for higher feed rate and depth of cut is in the range characteristic for conventional turning of carbon and alloy steels with the UCT higher than 20 μm.
- The ratio of uncut chip thickness to the cutting edge radius (h/r_β) describes the intensity of the ploughing action and can be used to distinguish between hard machining and conventional machining operations. In particular, the (h/r_β) ratio of about 0.3 was determined for the minimum h of 2.5 μm, which is close to the boundary between ploughing and cutting actions.
- The balance between the specific and ploughing energies (e_c/e_p) can be used to optimize hard machining operation.
- In order to minimize the energy consumption, finishing hard turning operations should not be performed with extremely low feed rates and depths of cut and larger tool nose radii.

References

1. Davim JP (2011) Machining of hard materials. Springer, London
2. Byrne G, Dornfeld D, Denkena D (2003) Advancing cutting technology. CIRP Ann Manuf Technol 52(2):483–507
3. Tönshoff HK, Arendt C, Ben Amor R (2000) Cutting of hardened steel. CIRP Ann Manufact Technol 49(2):547–566
4. Dornfeld D, Lee D-E (2008) Precision machining. Springer, New York
5. Chinchanikar S, Choudhury SK (2015) Machining of hardened steel—experimental investigations, performance modelling and cooling techniques: a review. Int J Mach Tools Manuf 89:95–109
6. Li JG, Lu Y, Zhao H, Li P, Yao YX (2014) Optimization of cutting parameters for energy saving. Int J Adv Manuf Technol 70(1–4):117–124
7. Mativenga PT, Rajemi MF (2011) Calculation of optimum cutting parameters based on minimum energy footprint. CIRP Ann Manufact Technol 60(1):149–152
8. Mayer R, Köhler J, Denkena B (2012) Influence of the tool corner radius on the tool wear and process forces during hard turning. Int J Adv Manuf Technol 58(9–12):933–940
9. Zhou JM, Walter H, Andersson M, Stahl JE (2003) Effect of chamfer angle on wear of PCBN cutting tool. Int J Mach Tools Manuf 43(3):301–305
10. Chou YK, Song H (2014) Tool nose radius effect on finish hard turning. J Mater Process Technol 148(2):259–268
11. Boothroyd G, Knight WA (2005) Fundamentals of machining and machine tools. Taylor & Francis, New York
12. Abrams premium steel. Steel guide. Internet at www.steel-guide.ue
13. Huang Y, Chou YK, Liang S (2007) CBN tool wear in hard turning: a survey on research progress. Int J Adv Manuf Technol 34(5):443–453
14. Grzesik W (2008) Advanced machining processes of metallic materials. Elsevier, Amsterdam